Electromagnetic analysis of specular resonance by periodic bilayer cylinders

Hiroyuki Ichikawa* and Uiko Nishimoto

Faculty of Engineering, Ehime University, 3 Bunkyo, Matsuyama 790-8577, Japan
*Corresponding author: ichikawa@ehime-u.ac.jp

Specular resonance by periodic bilayer cylinders is electromagnetically analyzed for the first time to our knowledge. The phenomenon occurs when the radius is roughly 0.8 times the wavelength. It is also discovered that the structure behaves as a good guided-mode resonant grating filter when the radius is around 0.4 times the wavelength.   © 2011 Optical Society of America

OCIS codes: 050.1755, 050.5745, 230.1950, 260.5740.

Optical elements composed of bilayer wavelength-sized dielectric spheres have been known to demonstrate strong specular reflection, e.g., they behave like mirrors, blazed gratings, or Bragg gratings [1–4] [Fig. 1(a)]. Its first experimental observation with a two-contacting sphere and subsequent numerical analysis in the microwave region date back to the 1980s [5–7]. Afterwards, we called the phenomenon *specular resonance* [7]. Miyazaki *et al.* have conducted extensive studies on the subject with structures up to clusters of bi- or trilayer spheres and found that specular resonance was observed only with bilayer structures [3,4]. As practical optical elements, the structures must be large enough to be treated as diffraction gratings rather than as just clusters of bilayer spheres.

This Letter first reports an electromagnetic numerical analysis of specular resonance by such bilayered structures. We employ freestanding one-dimensional gratings in the vacuum, composed of close-packed bilayer cylinders instead of spheres [Fig. 1(b)]. This is because accurate analysis of bilayer sphere gratings is difficult to conduct, as we suggest later. However, results with cylinder gratings provide quite useful information about fundamental properties. All numerical studies here assume cylinders of radius r and refractive index of 1.6, illuminated by a plane wave of 632.8 nm wavelength in the vacuum.

As a numerical tool, we employed the Fourier modal method (FMM) [8] with an S-matrix algorithm [9]. We believe that the popularly used finite-difference time-domain method is not accurate enough for this sort of structure and that the C method [10] has difficulty in handling vertical parts of the structure. The first task in the analysis is to determine how to slice the entire bilayer structure, because in the FMM, a continuous surface relief structure must be approximated with a staircase structure.
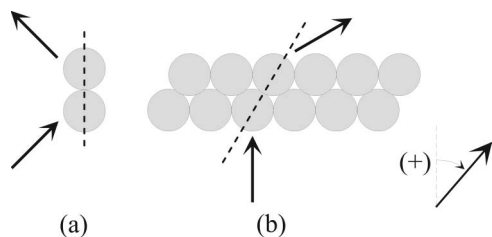
First, we investigated the convergence of three slicing strategies shown in Fig. 2, where the number of layers is $L = 10$, as an example. In strategy A, the entire structure is sliced into layers of equal thickness. In strategy B, the thickness of the layers of rapidly changing parts in the vertical direction, comprising 60% of the total thickness, is half the thickness of the other parts. In strategy C, thickness is determined so that the lateral difference of the widths of neighboring slabs is constant. As a typical result, convergence of total transmission efficiency, η^{T}, is shown in Fig. 3, where $r = 0.6\,\mu\mathrm{m}$, the incident angle $\theta = 0$, and the number of truncation orders $M = 50$ for the TE wave. The B-type slicing exhibits the best convergence, and the tendency is more or less the same for other θ and M. After trial computations with various L, M, and θ for $r = 0.6\,\mu\mathrm{m}$, we decided that the following conditions should be used afterwards: $L = 400$ and $M = 50$ for the TE wave and $L = 400$ and $M = 200$ for the TM wave for sufficient convergence, i.e., roughly of the orders of 10^{-4} for TE and 10^{-3} for TM.

Shown in Fig. 4 are transmission properties for $r = 0.4$, 0.6, and $2.0\,\mu\mathrm{m}$. Each thick line composed of blots denotes each diffraction order, and the color of the blot denotes the transmission efficiency of the mth order η_m^{T}. It is seen that strong diffraction is observed along the line connecting the points $(\theta, \theta_m) = (0, 60)$ and $(60, 0)$ for $r = 0.6$ and $2.0\,\mu\mathrm{m}$. This is indeed the evidence of the existence of specular resonance. According to computation with other values of r, the specular resonance occurs, roughly speaking, for $r \geq 0.5\,\mu\mathrm{m}$. This is because the

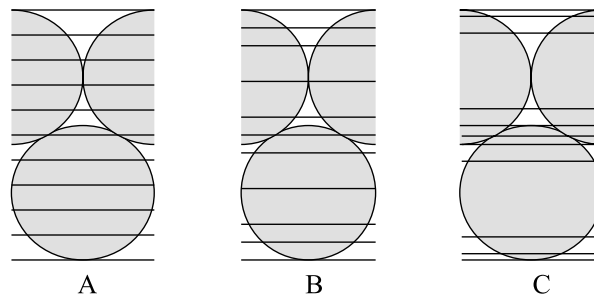Fig. 1.   Specular reflection by (a) a set of bispheres and (b) close-packed bilayer structures.

Fig. 2.   Slicing strategies, $L = 10$. A, equithickness; B, two-level thickness; C, variable thickness.
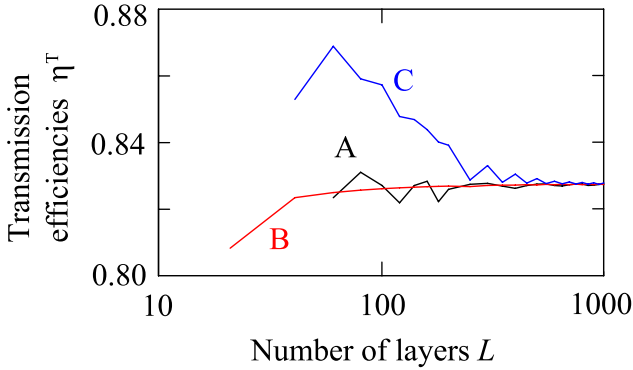
Fig. 3. (Color online) Convergence study. $r = 0.6\,\mu$m, $\theta = 0$ deg, $M = 50$.

specular resonance requires a suitable diffraction order that corresponds to each incident angle. The criterion in terms of a size parameter, $S = 2\pi r/\lambda > 5$, for the refractive index of 1.6 corresponds well with experimental observations by Miyazaki *et al.* [2]. The effect of specular resonance is noticeable in the example of $r = 2.0\,\mu$m. In Fig. 5, η_m^{T} is plotted against θ for $-5 \leq m \leq 5$, while actual propagating orders cover the range $-12 \leq m \leq 6$. It is remarkable to see that strong specular reflection exists at almost any incident angle in the range of $0 < \theta < 60$ deg.

It is worth mentioning that the specular resonance is more eminent with a large S, because there are more diffraction orders that match specular reflection. This might resemble the behavior of retroreflectors governed by the grating equation and geometrical reflection [11].

So far we have seen diffraction properties for close-packed bilayer cylinders, because the structure is the most practical. Next, let us look at properties for other structures, i.e., close-packed trilayer and simply stacked bi- and trilayer structures as shown in Fig. 6. The transmission properties are summarized in Fig. 7. In the case of simply stacked cylinders, the appearance of specular resonance will be found along the line connecting the points $(\theta, \theta_m) = (0, 0)$ and $(60, -60)$, if it exists. Indeed, there is one for the bilayer case. However, it is clearly shown that specular resonance does not occur for trilayer structures however cylinders are stacked.

The origin of specular resonance seems to be a combined effect of several causes. Here, we examine one of the candidates, i.e., Bragg diffraction. Obviously, the directions of diffracted plane waves are determined by the grating equation Eq. (1). If the incident and exit direc-
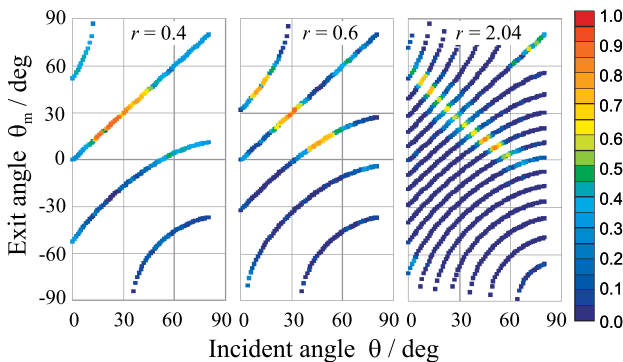
tions satisfy the Bragg condition, Eq. (2), the efficiency of the diffraction order would be high:

$$\sin\theta_m - \sin\theta = m\lambda/(2r), \qquad (1)$$

$$\sin\phi_j = j\lambda/(2\Lambda\tilde{n}_j), \qquad (2)$$

where Λ is Bragg depth, j denotes Bragg order, and $\tilde{n}_j$ is a sort of average refractive index which the jth Bragg order experiences as if there were a homogeneous medium.

Table 1 gives evaluated values of $\tilde{n}_j$ with properly chosen j for $1 \leq m \leq 4$ in the case of $r = 2\,\mu$m. The values for $-4 \leq m \leq -1$ are not listed, because the tendency is almost exactly the same. All $\tilde{n}_j$ in Table 1 are around 1.5, which are very likely values. We have to emphasize that any other value of j for each m is associated with either $\tilde{n}_j > 1.6$ or $\tilde{n}_j < 1.35$. This might be strong evidence of Bragg diffraction being the main cause of specular resonance. We encounter, however, a problem. The logic we have just employed to explain Bragg diffraction does not work for simply stacked structure. That is, there never exists a combination of m and j associated with a reasonable value of $\tilde{n}_j$. As a result, we can only state at this stage that multiple interference phenomena would cause the specular resonance, but not necessarily the Bragg diffraction.

Fig. 5. (Color online) TM transmission efficiencies for $r = 2.0\,\mu$m. Numbers in the graph denote m.

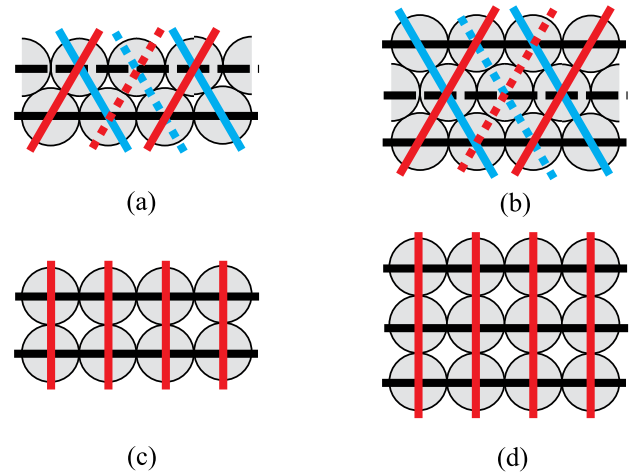Fig. 4. (Color online) TM transmission properties for $r = 0.4$, 0.6, and 2.0 μm.

Fig. 6. (Color online) Various structures considered. Colored lines denote planes for Bragg diffraction. (a) Close-packed bilayer, (b) close-packed trilayer, (c) simply stacked bilayer, (d) simply stacked trilayer.
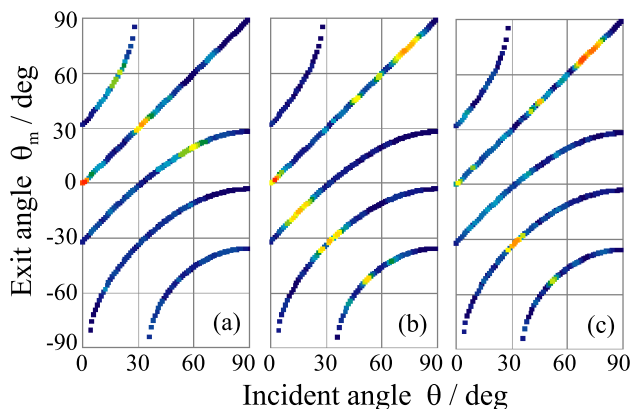
Fig. 7. (Color online) TM transmission properties for $r = 0.6\,\mu$m. (a) Close-packed trilayer, (b) simply stacked bilayer, (c) stacked trilayer.

Table 1. Candidates for Bragg Orders and Estimated $\tilde{n}_j$ for Close-Packed Cylinder of $r = 2\,\mu$m^a

m	1	2	3	4
θ	22.8	17.4	13.4	8.4
j	3	6	9	12
ϕ_j	7.2	12.6	16.6	21.6
ϕ_j	3.1	8.0	14.9	21.2
$\tilde{n}_j$	1.53	1.53	1.51	1.50

^{a}Units in degrees for angles.

Planes for multiple reflection are defined as in Fig. 6, among which red lines are associated with the specular resonance observed in Figs. 3–5 for $\theta \geq 0$. Cyan planes are associated with the case $\theta \leq 0$. Red and cyan planes are multilayered, although their sizes are narrow, and thus multiple interference works. On the other hand, black planes that would also contribute resonance are wide, but the number seems to be too few. Therefore, the resonance effect by the black planes is much weaker in bilayer structures than in trilayer ones, where the resonance caused by red and cyan planes is destroyed by that of black planes. This explains why the specular resonance occurs only with bilayer structures. By the way, planes defined by solid and dotted lines in Figs. 6(a) and 6(b) behave differently, which might cause the difference between close-packed and simply stacked layer structures.

It is interesting to see how close-packed bilayer cylinders with small radii, e.g., $2 \leq S \leq 3$, behave (Fig. 8). They certainly do not exhibit specular resonance, because only the zeroth diffraction order exists within meaningful incident angle range. Instead, extremely sharp drops are observed, i.e., alternatively sharp reflection peaks: FWHMs of the narrowest peaks are 0.04 and 0.25 deg for the TE and TM waves, respectively. This is due to
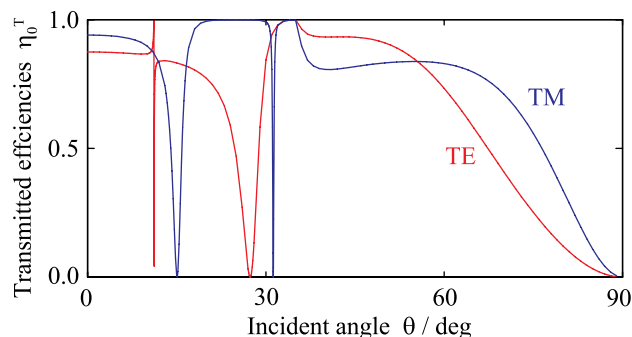

Fig. 8. (Color online) Transmission efficiencies for close-packed bilayer cylinders with $r = 0.2\,\mu$m.

the fact that the bilayer cylinders are considered an asymmetrical three-core waveguide, which behaves as a guided-mode resonant grating filter. It is not so easy to predict the behavior of bilayer cylinders, because the structure is a bit more complicated than that of conventional ones.

In summary, the transmission properties of bilayer cylinders are investigated, and experimental observation of specular resonance is well explained. However, the origin of the phenomenon is not as simple as Bragg diffraction, and a full explanation is left to future study. A byproduct of the present study is that bilayer cylinders are found to behave as good guided-mode resonant grating filters, which are far less demanding to fabricate than conventional ones requiring lithography. We believe that we could show that close-packed cylinders or spheres can be attractive enough optical elements for many applications despite the relative limitation of design freedom.

References
1. H. T. Miyazaki, H. Miyazaki, and K. Miyano, Opt. Lett. **27**, 1208 (2002).
2. H. T. Miyazaki, H. Miyazaki, and K. Miyano, J. Opt. Soc. Am. A **20**, 1771 (2003).
3. H. T. Miyazaki, H. Miyazaki, N. Shinya, and K. Miyano, Appl. Phys. Lett. **83**, 3662 (2003).
4. H. T. Miyazaki, H. Miyazaki, Y. Jimba, Y. Kurokawa, N. Shinya, and K. Miyano, J. Appl. Phys. **95**, 793 (2004).
5. R. T. Wang, J. M. Greenberg, and D. W. Schuerman, Opt. Lett. **6**, 543 (1981).
6. G. W. Kattawar and C. E. Dean, Opt. Lett. **8**, 48 (1983).
7. K. A. Fuller, G. W. Kattawar, and R. T. Wang, Appl. Opt. **25**, 2521 (1986).
8. J. Turunen, in *Micro-Optics*, H. P. Herzig, ed. (Taylor & Francis, 1997), pp. 31–52.
9. L. Li, J. Opt. Soc. Am. A **13**, 1024 (1996).
10. L. Li, J. Chandezon, G. Granet, and J.-P. Plumey, Appl. Opt. **38**, 304 (1999).
11. H. Ichikawa, J. Opt. A **6**, S121 (2004).